0013-7227/02/$15.00/0
Printed in U.S.A.

The Journal of Clinical Endocrinology & Metabolism 87(8):3902–3910

Glucose Uptake and Perfusion in Subcutaneous and Visceral Adipose Tissue during Insulin Stimulation in Nonobese and Obese Humans

KIRSI A. VIRTANEN, PETER LÖNNROTH, RIITTA PARKKOLA, PAULIINA PELTONIEMI, MARKKU ASOLA, TAPIO VILJANEN, TUULA TOLVANEN, JUHANI KNUUTI, TAPANI RÖNNEMAA, RISTO HUUPPONEN, AND PIRJO NUUTILA

Turku PET Centre (K.A.V., P.P., M.A., T.V., T.T., J.K., P.N.), Departments of Radiology (R.P.), Medicine (M.A., T.R., P.N.), Pharmacology and Clinical Pharmacology (R.H.), University of Turku, Turku University Central Hospital, Turku 20521, Finland; and Department of Medicine (P.L.), University of Gothenburg, Gothenburg 41345, Sweden

To elucidate the role of adipose tissue glucose uptake in whole-body metabolism, sc and visceral adipose tissue glucose uptake and perfusion were measured in 10 nonobese and 10 age-matched obese men with positron emission tomography using [^{18}F]-2-fluoro-2-deoxy-D-glucose, and [^{15}O]-labeled water during normoglycemic hyperinsulinemia. Whole-body and skeletal muscle glucose uptake rates per kilogram were lower in obese than in nonobese subjects ($P < 0.01$). Compared with nonobese, the obese subjects had 67% lower abdominal sc and 58% lower visceral adipose tissue glucose uptake per kilogram of fat. In both groups, insulin stimulated glucose uptake per kilogram fat was significantly higher in visceral fat depots than in sc regions ($P < 0.01$). Both sc and visceral adipose tissue blood flow expressed per kilogram and minute was impaired in the obese subjects, compared with the nonobese ($P < 0.05$). Fat masses measured with magnetic resonance images were higher in obese than in nonobese individuals. If regional glucose uptake rates were expressed as per total fat mass, total glucose uptake rates per depot were similar in obese and nonobese subjects and represented 4.1% of whole-body glucose uptake in obese and 2.6% in nonobese subjects ($P < 0.02$ between the groups). In conclusion, insulin-stimulated glucose uptake per kilogram fat is higher in visceral than in sc adipose tissue. Glucose uptake and blood flow in adipose tissue exhibit insulin resistance in obesity, but because of the larger fat mass, adipose tissue does not seem to contribute substantially to the reduced insulin stimulated whole-body glucose uptake in obesity. (*J Clin Endocrinol Metab* 87: 3902–3910, 2002)

SKELETAL MUSCLE IS the major site for insulin-stimulated glucose uptake *in vivo* (1, 2). Besides myocytes, adipocytes are also highly insulin-responsive cells. Until recently, the major role of adipose tissue has been mostly regarded as lipid storage and mobilization. Accumulation of fat in the abdominal adipose tissue region is believed to be significant in the pathogenesis of insulin resistance syndrome (3–7). Enlargement of the adipose cells is accompanied by high concentration of FFA in plasma and increased rate of fat oxidation leading to inhibition of glucose oxidation (8).

In obese subjects, resistance to the effect of insulin to enhance glucose uptake in the adipose tissue has been demonstrated *in vitro*. The insulin receptor density is decreased (9, 10) and the glucose transport system is less effective because of a reduced number of glucose transporters in the intracellular pool (11). Moreover, the ability of insulin to stimulate triglyceride synthesis and inhibit lipolysis in adipose tissue is impaired in obesity (12). Although there is clear mechanistic evidence for insulin resistance in adipocytes, it is, however, still not clear to what extent this contributes to whole-body resistance to insulin-stimulated glucose uptake in obese subjects.

Abbreviations: BMI, Body mass index; [^{18}F]FDG, [^{18}F]fluoro-deoxy-glucose; LC, lumped constant; MRI, magnetic resonance imaging; PET, positron emission tomography; ROI, region(s) of interest.

Studies on the effects of obesity on adipose tissue glucose metabolism and perfusion *in vivo* have given controversial results. When radioactive [^{14}C]glucose was given with glucose either intravenously (13) or orally (14), its incorporation into sc adipose tissue was 1–4% of given glucose in lean individuals, and the incorporation was increased in the obese subjects (up to 20%) (13, 14). In the study by Coppack *et al.* (15) in which postprandial adipose glucose uptake was estimated using A-V differences and the ^{133}Xe clearance technique, no differences between lean and obese subjects were found in glucose uptake per adipose tissue weight, although adipose tissue blood flow was 50% lower in the obese subjects. *In vivo* measurement of adipose tissue glucose metabolism using microdialysis showed evidence for substantial production of lactate in the sc adipose tissue (16, 17) and increased lactate production in obese subjects (18). Intraabdominal fat depots cannot be reached by these methods. Thus, because of methodological limitations, the role of various adipose tissue depots for whole-body glucose homeostasis in insulin-resistant conditions is not yet clarified.

Positron emission tomography (PET), in combination with [^{18}F]fluoro-deoxy-glucose ([^{18}F]FDG) and [^{15}O]-labeled water allows noninvasive quantification of tissue specific glucose uptake and perfusion. This technique has been used in studies of skeletal muscle and myocardial glucose metabolism and perfusion *in vivo* (19–21). We have recently shown evidence for insulin resistance in sc adipose tissue in obesity

(22) in a study in which sc adipose tissue glucose uptake was measured simultaneously with [^{18}F]FDG-PET and microdialysis technique combined with perfusion measurement with [^{15}O]-labeled water. The present study was designed to compare insulin-stimulated glucose uptake and perfusion rates in sc and visceral adipose tissue and skeletal muscle in obese and nonobese subjects to clarify the contribution of adipose tissue to total body glucose homeostasis and the insulin resistance in obesity.

Subjects and Methods

Subjects

Ten obese [age 25–40 yr, body mass index (BMI) 27–34 kg/m^2, waist to hip ratio >1.0] and 10 nonobese age-matched (BMI 19–24 kg/m^2, waist to hip ratio <1.0) males were recruited for the study. The characteristics of the study subjects are shown in Table 1. The subjects were healthy as judged by history, physical examination, and routine laboratory tests, and they were not taking any medications. The nature, purpose, and potential risks of the study were explained to all subjects before they gave their written informed consent to participate. The Joint Commission of Ethics of the University of Turku and Turku University Central Hospital approved the study. The study was conducted according to Declaration of Helsinki principles.

Study design

The design of the study is shown in Fig. 1. Studies were performed after an overnight fast. Caffeine and nicotine were prohibited for 24 h before the study. Alcohol consumption and fatty meals were avoided for 3 d, and strenuous physical activity was not allowed for 48 h before the study. All studies were performed in the supine position. Two catheters were inserted, one in a left hand antecubital vein for infusion of glucose and insulin and injections of [^{15}O]H_2O and [^{18}F]FDG, and another in the radial artery in the right hand for blood sampling. Each study consisted of a 130-min euglycemic hyperinsulinemic (1 mU/kg·min^{-1}) period. During hyperinsulinemia, normoglycemia was maintained by a variable infusion rate of 20% glucose based on arterial plasma glucose determinations. Forty-five minutes after the start of the clamp, blood flow was measured in the abdominal region using [^{15}O]H_2O. A dose of 1.2–1.3 GBq [^{15}O]H_2O was injected iv and dynamic scanning was performed for 6 min (6 × 5 sec, 6 × 15 sec, 8 × 30 sec frames). To determine the input function, blood from the radial artery was continuously withdrawn using a pump at a speed of 6 ml/min. The radioactivity concentration was measured using a two-channel detector system (Scanditronix, Uppsala, Sweden) calibrated to an automatic gamma counter (Wizard 1480, Wallac, Inc., Turku, Finland) and the PET scanner. At 60 min the dose of 0.18–0.19 GBq [^{18}F]FDG was injected iv over 60 sec and a 50-min dynamic scan of abdomen, the navel as the midpoint level, was simultaneously started (2 × 30 sec, 4 × 60 sec, 9 × 300 sec frames). Thereafter, a femoral dynamic scan, the middle of a thigh selected for the midpoint level, for 20 min (6 × 180 sec) was performed. Arterial blood samples for the measurement of plasma radioactivity were withdrawn once during each time frame and measured using the automatic gamma counter. Blood samples for the measurement of serum insulin and FFA and plasma lactate concentrations were taken every 30 min of the clamp study.

Production of PET tracers

Production of [^{15}O] ($t_{1/2}$ = 123 sec) was accomplished with a low-energy deuteron accelerator Cyclone 3 (Ion Beam Application Inc., Louvain la-Neuve, Belgium). [^{15}O]H_2O was produced based on the membrane technique (23) using sterile exchangeable tubing in the device. An online radioactivity recording for each administration of [^{15}O]H_2O was performed for each examination with a detector cross-calibrated to dose calibrator (VDC404, Instrumenten, AC Joure, The Netherlands). Pyrogenicity tests were performed once a month to verify the purity of the product. [^{18}F]FDG ($t_{1/2}$ = 109 min) was synthesized with an automatic apparatus by a modified method of Hamacher *et al.* (24). The specific radioactivity at the end of the synthesis was more than 75 GBq/μmol, and the radiochemical purity exceeded 98%.

Image acquisition and processing

The subjects were positioned supine in a 15-slice ECAT 931/08-tomograph (Siemens/CTI Inc., Knoxville, TN). Technical in-plane resolution was 6.5 mm and axial resolution was 6.7 mm in the scanner. Before the emission scans, 5-min transmission scans in abdominal and femoral regions were performed for measuring photon attenuation with a removable ring source containing ^{68}Ge. All data were corrected for dead time, decay, and measured photon attenuation and reconstructed in a 128 × 128 matrix. For image processing, a recently developed Bayesian iterative reconstruction algorithm using median root prior with 150 iterations and the Bayesian coefficient of 0.3 was applied (25, 26). PET counts were converted to radioactivity concentration values (becquerel per milliliter) using a calibration factor derived from phantom studies.

Regions of interest (ROI)

The ROI were drawn on magnetic resonance imaging (MRI) scans and were located in sc, visceral, and perirenal regions in the abdominal area and in the sc adipose tissue in femoral region. The ROI were copied to the [^{15}O]H_2O and the [^{18}F]FDG images to cross-sectional slices from identical regions as presented in Fig. 2. In the femoral region, ROI were additionally drawn in the anteromedial muscle compartments in four cross-sectional slices, carefully avoiding large blood vessels (19). Localization of the muscle compartments was verified by comparing the [^{18}F]FDG images with the MRI scans in the same plane.

TABLE 1. Characteristics of the study subjects

	Nonobese (n = 10)	Obese (n = 10)	*P* (*t* test)
Age (yr)	29.5 ± 1.6	31.6 ± 1.5	NS
Body weight (kg)	73.3 ± 3.0	100.4 ± 3.6	<0.001
BMI (kg/m^2)	22.7 ± 0.5	29.9 ± 0.9	<0.001
Waist/hip ratio	0.96 ± 0.01	1.05 ± 0.02	<0.001
Body fat %	16 ± 1	27 ± 1	<0.001
Plasma glucose (mmol/liter)	5.3 ± 0.1	5.1 ± 0.1	NS
Serum insulin (pmol/liter)	29 ± 3	59 ± 7	<0.001
Serum total cholesterol (mmol/liter)	4.5 ± 0.3	4.5 ± 0.4	NS
Serum triglycerides (mmol/liter)	0.8 ± 0.2	1.4 ± 0.3	<0.05
Serum HDL cholesterol (mmol/liter)	1.3 ± 0.1	1.1 ± 0.1	NS
Serum LDL cholesterol (mmol/liter)	2.8 ± 0.3	2.8 ± 0.3	NS
Serum FFA (mmol/liter)	0.59 ± 0.05	0.57 ± 0.05	NS
Plasma lactate (mmol/liter)	0.7 ± 0.1	0.8 ± 0.1	NS
Serum leptin (ng/ml)	2.3 ± 0.3	8.6 ± 1.7	<0.001

Plasma and serum concentrations were measured during fasting state. HDL, High-density lipoprotein; LDL, low-density lipoprotein; FFA, free fatty acid.

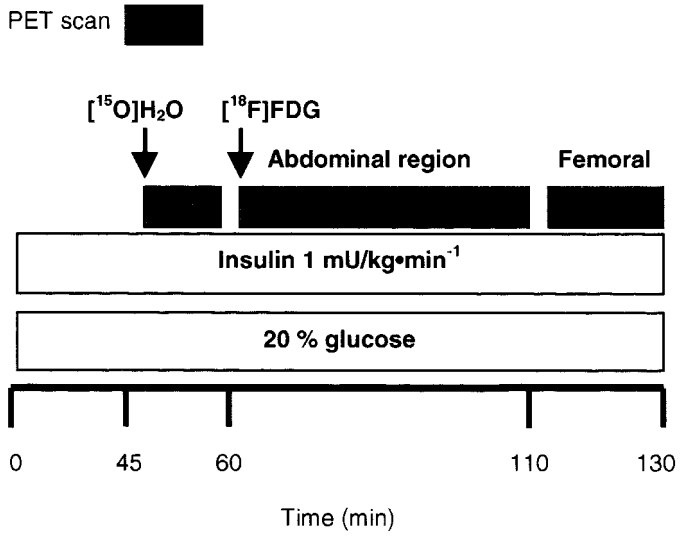

FIG. 1. Study design. *Black arrows* indicate the time points of positron emitting tracer ($[^{15}O]H_2O$ and [18F]FDG) injections. *Shaded rectangles* denote the time period of dynamic scanning.

Measurement of adipose tissue blood flow

The arterial input curve was corrected for dispersion and delay, as previously described (27). The autoradiographic method, a 250-sec integration time and partition value of 0.19 for adipose tissue, was applied to calculate blood flow pixel by pixel, as previously described (22, 27).

Measurement of adipose tissue and skeletal muscle glucose uptake

The three-compartment model of [18F]FDG kinetics was used as described earlier (19). After transport into the cell, [18F]FDG is phosphorylated by hexokinase and trapped (19, 28). The fractional rate of tracer uptake was quantified by using graphical analysis of plasma and tissue (adipose tissue/skeletal muscle) time-activity curves (29). Linear regression was used to determine the slope of the time-activity points between min 10 and 40 in abdominal area and between min 50 and 70 in femoral area after [18F]FDG injection. The rate of regional glucose uptake measured using [18F]FDG was calculated by multiplying fractional [18F]FDG uptake by plasma glucose concentration $[Glc]_p$ and divided this by lumped constant (LC) value of 1.2 in muscle (30) and LC value of 1.14 in adipose tissue (22). LC is a correction factor, which accounts for difference in transport and phosphorylation between [18F]FDG and glucose. We have recently shown that LC for [18F]FDG in adipose tissue is 1.14 (22).

MRI

The abdominal and femoral regions were imaged with a 0.23 T Outlook GP (Marconi Medical Systems Inc., Cleveland, OH) magnetic resonance imager using a body coil. Transverse T1-weighted field echo images with time repetition of 124 msec and time echo of 5 msec were obtained with the same pixel size as the PET images (128 × 128). The level of the midslice and the upper and lower border of the area imaged were drawn on the skin of the subjects and the same imaging area was used in PET imaging to confirm congruent data between PET and MRI. On T1-weighted MR images, the adipose tissue is recognized as white, skeletal muscle as gray, water as dark gray, and bones and fast blood flow in vessels as black (Fig. 2). Intraabdominal fat was divided into visceral and retroperitoneal fat by delineation along the dorsal borderline of the intestines and the ventral surface of the kidneys. Adipose tissue masses in abdominal region were measured as earlier described by Abate *et al.* (31).

Whole-body glucose uptake

Whole-body glucose uptake as the glucose disposal rate was determined using the euglycemic hyperinsulinemic clamp technique, as previously described (32). The rate of whole-body glucose uptake was calculated during the same period that the measurements of adipose tissue blood flow and glucose uptake were performed.

Biochemical analyses

Arterial and plasma glucose was determined in duplicate by the glucose oxidase method (Analox GM9 Analyzer, Analox Instruments, London, UK). Serum insulin concentrations were measured basally (fasting) and at 30-min intervals during insulin infusion using a double-antibody RIA (Phadeseph Insulin RIA kit, Pharmacia & Upjohn, Uppsala, Sweden) with a detection limit of 15 pmol/liter. Plasma lactate and total serum cholesterol, triglycerides, and high-density lipoprotein cholesterol were measured using standard enzymatic methods (Roche Molecular Biochemicals, Mannheim, Germany) with a fully automated analyzer (Hitachi 704, Hitachi, Tokyo, Japan). Low-density lipoprotein serum cholesterol was calculated according to the equation by Friedewald (33). Serum FFA were determined by an enzymatic method (ACS-ACOD method, Wako Chemicals, Neuss, Germany). Serum leptin was assayed by means of a ^{125}I RIA kit for human leptin (Linco Research, Inc., St. Charles, MO).

Anthropometric measurements

Height and weight were measured by standard procedures. Waist and hip circumferences were measured at the level midway between lowest rib and iliac crest in the midaxillary line and at the maximum circumference in the hip area in all subjects by the same investigator. Body fat content was estimated from four skinfolds (subscapular, triceps brachii, biceps brachii, and crista iliaca) as measured with caliper (34).

Statistical analyses

Results are expressed as the mean ± SEM. Statistical calculations were performed using the SAS statistical program package (SAS Institute, Inc., Cary, NC). Differences between the two groups were compared using a *t* test. One-way ANOVA was carried out to compare differences between adipose tissue depots. Pearson's correlation coefficients were calculated where appropriate. A two-tailed *P* value less than 0.05 was regarded as statistically significant.

Results

Metabolic characteristics during the studies

Fasting plasma glucose values were similar in both groups, but concentration of fasting serum insulin, triglycerides, and leptin were higher in the obese than in the nonobese subjects (Table 1). During euglycemic hyperinsulinemic clamp, plasma glucose concentrations averaged 4.9 ± 0.1 mmol/liter in both groups. Serum insulin concentrations were higher in the obese than in the nonobese subjects (475 ± 22 *vs.* 383 ± 21 pmol/liter, $P < 0.05$). Serum FFA concentrations were decreased in both groups by insulin but remained higher in the obese, compared with the nonobese. During insulin infusion, plasma lactate concentration increased slightly in the nonobese but not in the obese subjects (difference in the change between groups: $P < 0.05$).

Adipose tissue glucose uptake

In nonobese subjects, the rate of insulin stimulated glucose uptake per kilogram tissue was higher in visceral and perirenal fat depots (32.7 ± 3.5 and 30.0 ± 3.8 μmol/kg·min^{-1}) than in sc adipose tissue (16.7 ± 3.4 μmol/kg·min^{-1}, $P < 0.05$, sc *vs.* visceral or perirenal), but glucose uptake rates in abdominal and femoral sc areas were not different (Fig. 3). During hyperinsulinemic clamp, rates of adipose tissue glucose uptake per kilogram tissue were 67% lower in abdom-

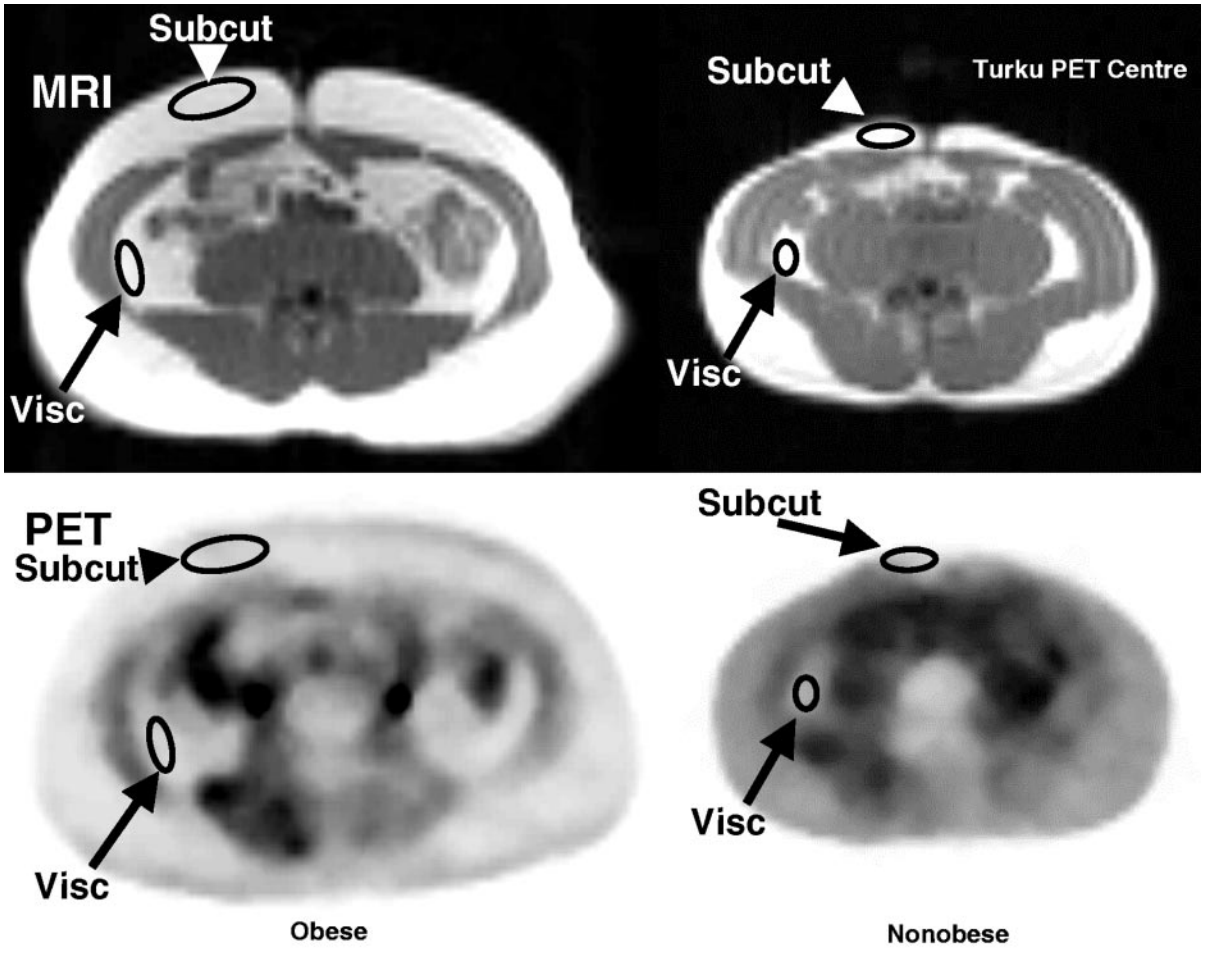

FIG. 2. An example of MRI and [^{18}F]FDG-PET images in the abdominal region of a nonobese (*right*) and an obese subject (*left*). ROI are outlined with *black* in sc adipose tissue (subcut) and in visceral adipose tissue (visc). MRI and PET images are from the same level. In the lower panel are the PET images in which the highest activity is shown as *black* as an index of trapping.

inal sc, 58% lower in visceral, and 63% lower in perirenal adipose tissue ($P < 0.01$ obese *vs.* nonobese in all depots, Fig. 3). In obese subjects, the rate of insulin-stimulated glucose uptake per mass unit was more than 2-fold higher in visceral and perirenal adipose tissue than in sc fat (13.6 ± 1.3, 11.2 ± 1.9 *vs.* 5.6 ± 0.5 μmol/kg·min^{-1}, $P < 0.05$, Fig. 3).

Whole-body and skeletal muscle glucose uptake

Whole-body glucose uptake as the glucose disposal rate was measured during hyperinsulinemia. Compared with lean subjects, obese subjects had 49% lower whole-body glucose uptake (19.7 ± 2.8 *vs.* 38.4 ± 3.2 μmol/kg·min^{-1}, obese *vs.* nonobese, $P < 0.01$, Fig. 3) and 45% lower skeletal muscle glucose uptake measured using [^{18}F]FDG-PET (31 ± 6 *vs.* 56 ± 7 μmol/kg muscle·min^{-1}, respectively, $P < 0.01$, Fig. 3).

Adipose tissue mass

Abdominal adipose tissue mass measured with MRI was significantly larger in the obese than in the nonobese subjects in all abdominal depots (Fig. 4.). In both groups, abdominal sc adipose tissue mass was 4-fold larger than the visceral fat mass.

Relationship between adipose tissue and whole-body glucose uptake

When adipose tissue glucose uptake per mass unit was multiplied by the adipose tissue mass and the uptake expressed per total abdominal adipose tissue, no differences could be found between the obese and the nonobese (Fig. 4). There was an inverse relationship between fat mass in sc and visceral depots and the corresponding regional glucose uptake rates per mass unit ($r = -0.57$, $P = 0.009$ in sc adipose tissue and $r = -0.71$, $P = 0.0007$ in visceral adipose tissue, Fig. 5). Because the obese subjects had lower whole-body uptake rates and enlarged body fat masses, the relative contribution of abdominal adipose tissue compartments to the whole-body glucose uptake was greater in the obese (4.1% ± 0.5%), compared with the nonobese subjects (2.6% ± 0.4%, $P < 0.02$, obese *vs.* nonobese). Insulin-stimulated skeletal muscle glucose uptake measured with [^{18}F]FDG-PET correlated linearly and closely with whole-body glucose uptake measured by means of the insulin clamp method (Fig. 6). Furthermore, visceral adipose tissue insulin-stimulated glucose uptake rates correlated significantly with whole-body glucose uptake (Fig. 6). Consequently, visceral adipose tissue

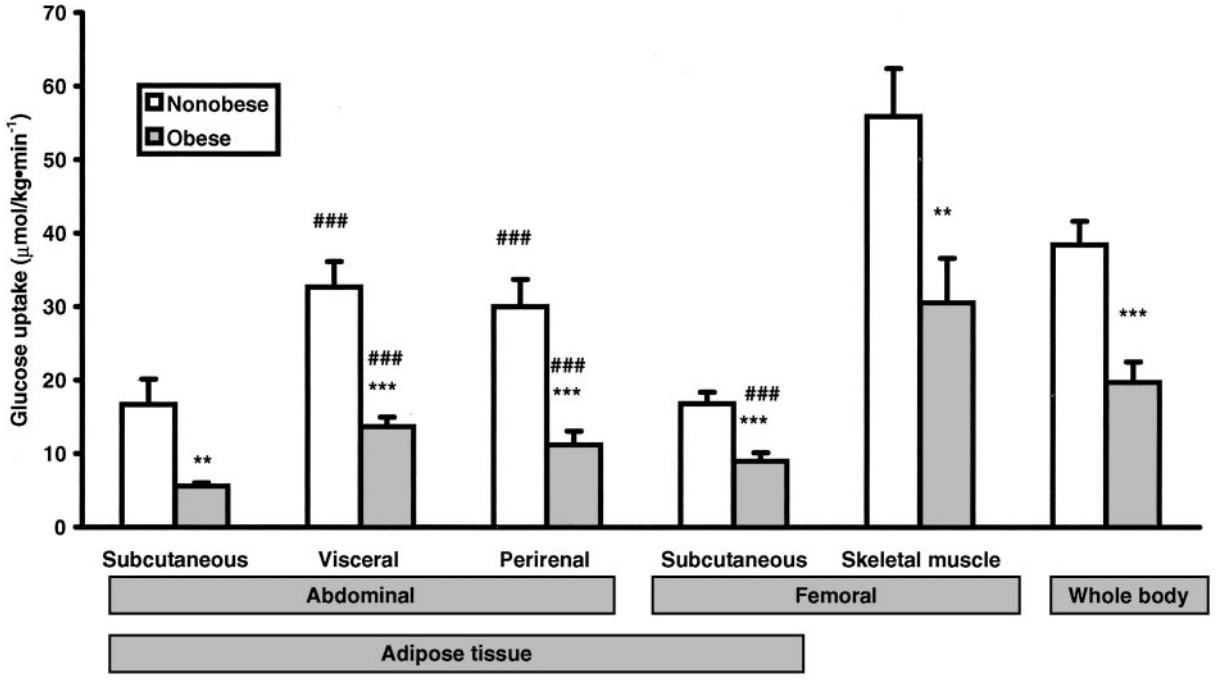

FIG. 3. Glucose uptake in adipose tissue depots and skeletal muscle measured with [^{18}F]FDG-PET and whole-body glucose disposal measured with insulin clamp in the nonobese (□) and obese (▨) subjects. **, $P < 0.01$ obese *vs.* nonobese; ***, $P < 0.001$ obese *vs.* nonobese; ###, $P < 0.01$, compared with abdominal sc adipose tissue.

insulin-stimulated glucose uptake correlated with skeletal muscle glucose uptake in the pooled data. Also, a significant correlation between abdominal sc adipose tissue glucose uptake and whole-body glucose uptake (M value) during insulin-stimulated (clamp) conditions was found (r = 0.55, $P = 0.01$).

Adipose tissue blood flow

Rates of insulin-stimulated adipose tissue blood flow per kilogram tissue were lower in the obese than in the nonobese subjects in all abdominal fat depots ($P < 0.05$ in all depots, Table 2). Blood flow rate per kilogram tissue was highest in visceral adipose tissue in all subjects but was not statistically different from sc or perirenal adipose tissue. When adipose tissue perfusion was expressed as per total fat mass in abdominal region, the obese had higher sc and visceral perfusion per depot than the nonobese subjects ($P < 0.05$, obese *vs.* lean, Fig. 4). Insulin-stimulated adipose tissue glucose uptake rates correlated with the rates of insulin-stimulated adipose tissue blood flow in abdominal sc adipose tissue (r = 0.60, $P < 0.01$) and visceral adipose tissue (r = 0.55, $P < 0.05$) in the pooled data.

Discussion

The present data show that insulin-resistant obese subjects have markedly decreased adipose tissue glucose uptake rates per kilogram of tissue during insulin stimulation both in visceral and sc fat depots, compared with the nonobese subjects. However, because of enlargement of the fat mass, the total amount of glucose taken up by abdominal fat depots is not reduced in the obese. Importantly, our data confirm that metabolic activity in visceral adipose tissue is higher than that in the sc depot both in the nonobese and obese subjects.

Previously, isolated adipocytes of obese individuals and patients with diabetes have been shown to be insulin resistant (16, 35, 36), whereas the results obtained *in vivo* have been heterogeneous (13–15). In the present study, glucose uptake per tissue mass was about 60% lower in obese than in lean subjects in all fat regions measured. Adipose tissue glucose uptake per kilogram tissue was slightly lower in abdominal sc areas, compared with the femoral region in the obese but not in the nonobese subjects. In accordance with earlier studies (1, 30, 37), the obese subjects exhibited skeletal muscle insulin resistance and the glucose disposal rate was decreased indicating whole-body insulin resistance (Fig. 3). Moreover, the rates of whole-body glucose disposal correlated directly with the glucose uptake both in skeletal muscle and adipose tissue.

Because rates of insulin-stimulated glucose uptake were measured with [^{18}F]FDG-PET in a volume or mass unit of the tissue, associations between metabolic rates and fat masses could be studied. Glucose uptake per kilogram tissue was inversely and curvilinearly correlated with fat mass demonstrating a minimum uptake rate per mass unit at sc and visceral fat masses above approximately 4 and approximately 1 kg, respectively (Fig. 5). This might reflect the loss of insulin action on glucose transport and postreceptor functions in adipocytes found in obese subjects (38, 39) and suggests that a continuous inhibition of the glucose uptake in the expanding cell until its minimum level is reached. However, when we thereafter calculated the adipose tissue glucose uptake rate as per the total fat depot, the regional glucose uptake per depot in sc, visceral, and perirenal regions turned

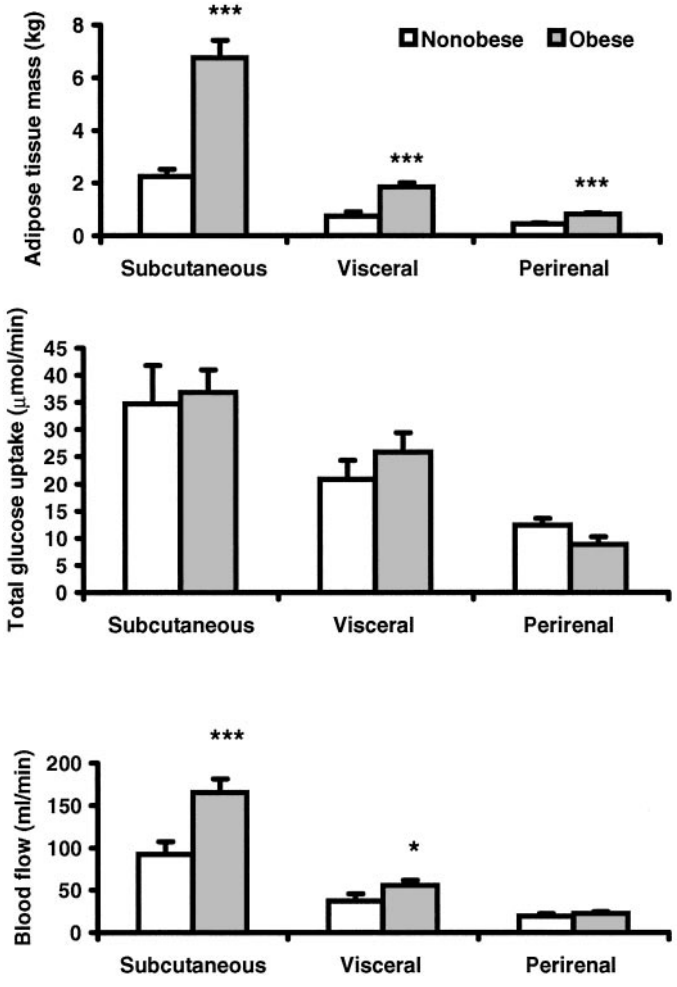

FIG. 4. Abdominal adipose tissue mass, insulin stimulated glucose uptake and blood flow in nonobese (□) and in obese (▨) *subjects*. Glucose uptake and blood flow values are expressed per whole fat depot. *, $P < 0.05$ obese *vs.* nonobese; ***, $P < 0.001$ obese *vs.* nonobese.

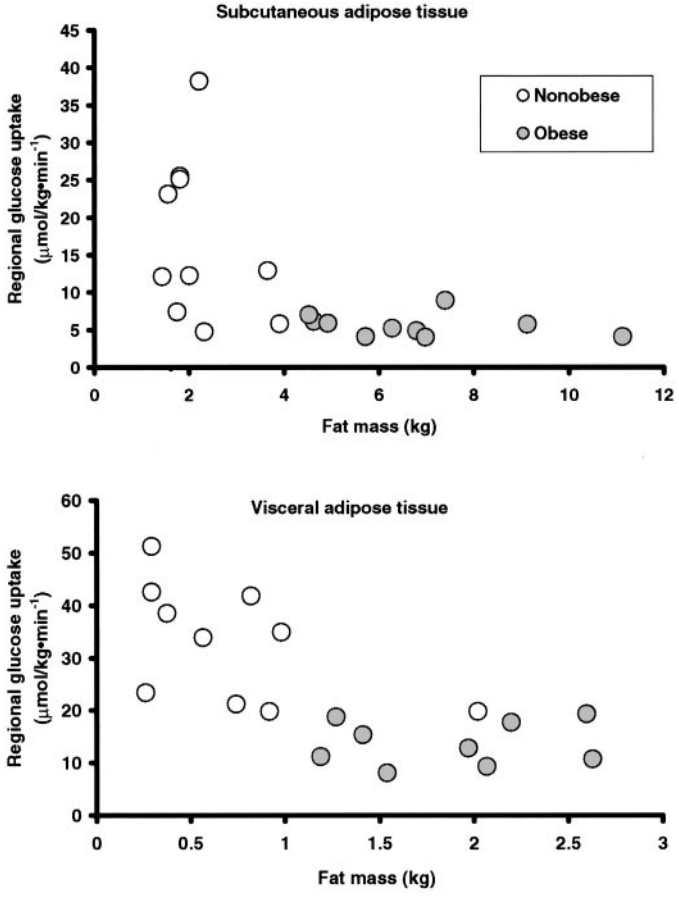

FIG. 5. Regional adipose tissue insulin-stimulated glucose uptake plotted against fat mass. $r = -0.57$, $P < 0.01$ in abdominal sc adipose tissue; $r = -0.71$, $P < 0.001$ in visceral adipose tissue.

out to be surprisingly similar in the obese and nonobese subjects (Fig. 4).

Although the total amount of glucose taken up by abdominal adipose depots was similar in the obese and nonobese subjects, its relative proportion of whole-body glucose uptake was different. The proportion of glucose taken up in abdominal sc (2% *vs.* 1.3%, obese *vs.* nonobese, $P < 0.05$) and visceral areas (1.6% *vs.* 0.8%, respectively, $P < 0.05$) relative to the whole-body glucose uptake was higher in the obese than nonobese subjects. For the estimation of whole-body fat mass, we used skinfold measurements (34). If we assume that the nonabdominal adipose tissue consists mainly of sc adipose tissue with glucose uptake rates per kilogram tissue similar to those of femoral sc adipose tissue, the average glucose uptake in total body adipose tissue (abdominal plus rest of the fat) would be 8% in the nonobese subjects and 13% in the obese subjects of the given glucose during the clamp. In the nonobese subjects, this is more than previously suggested (40), whereas in the obese subjects, it is in the same magnitude as earlier shown (14, 40).

The obese subjects had clearly higher plasma insulin concentrations during the clamp period than the lean subjects, probably reflecting their basal hyperinsulinemia or decreased insulin clearance (41, 42). Because of this difference in insulin concentration, the insulin resistance of the adipose tissue in obese subjects may be even higher than suggested in the present study. Suppression of hepatic glucose production has been shown to be effective at the plasma insulin levels used in the present study (43, 44).

Insulin-stimulated glucose uptake rate per tissue mass was higher in visceral adipose tissue, compared with sc depot, regardless of the magnitude of obesity. Lipid uptake and mobilization have also been demonstrated to be more active in intraabdominal fat (5), indicating a more active metabolic role of visceral than sc fat depot. One reason for higher glucose uptake per tissue mass in visceral adipose tissue in comparison with sc adipose tissue may be different sizes of the adipocytes in these depots; visceral adipocytes are smaller than sc, and visceral fat contains more adipocytes per gram than sc fat (45), which may facilitate glucose uptake. The mass of sc adipose tissue was, on average, 4-fold the mass of the visceral depot in both groups. Therefore, despite the fact that the intraabdominal visceral adipose tissue is metabolically more active than sc adipose tissue per tissue weight, the large sc adipose tissue depot is more important to whole-body glucose metabolism.

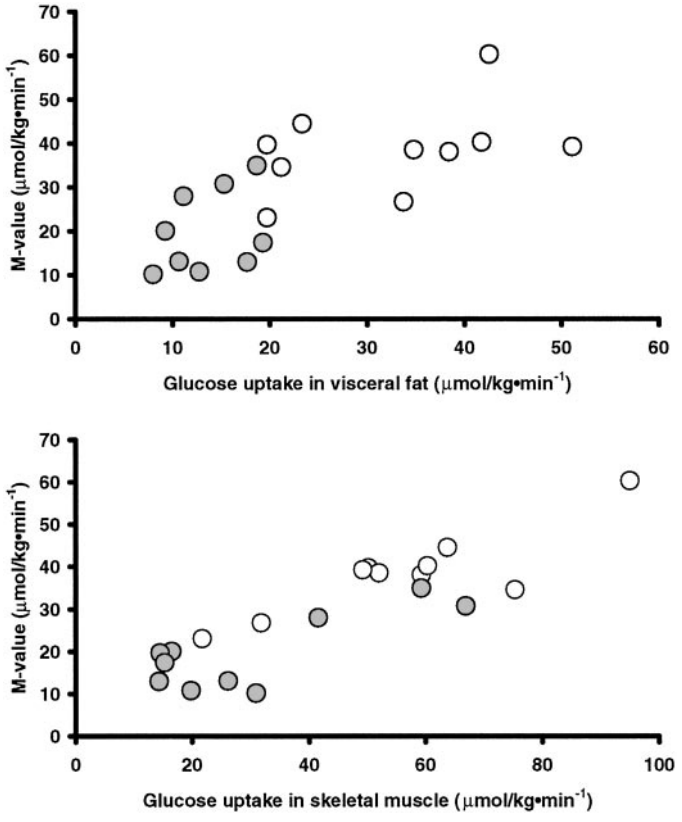

FIG. 6. Correlation between visceral adipose tissue and whole-body insulin stimulated glucose uptake (M value) and skeletal muscle and whole-body insulin stimulated glucose uptake (M value). Obese subjects are shown as ●, and nonobese subjects as ○. Coefficients for correlation were calculated using Pearson's correlation test. In the pooled data, coefficient for correlation between M value and glucose uptake in visceral adipose tissue was $r = 0.71$, $P < 0.001$ and between M value and glucose uptake in skeletal muscle it was $r = 0.86$, $P < 0.001$.

Adipose tissue perfusion per kilogram tissue was decreased in obese subjects both in sc and visceral fat depots. Decreased adipose tissue blood flow rates have been reported earlier in obese subjects (12, 46, 47). The thicker layer of sc adipose tissue in obese subjects could partly explain the lower rates of adipose tissue blood flow (48). Although adipose tissue perfusion per adipose mass was significantly decreased in obese, total blood flow per total adipose fat depot was higher in obese than in nonobese in sc and visceral areas (Fig. 4). This implies that perfusion is relatively more preserved than glucose uptake during the enlargement of adipose fat depot. It has been speculated that the delivery of insulin and glucose to the adipose tissue may be impaired in obesity and that this may, in part, explain the prevailing insulin resistance. However, interstitial concentrations of glucose and insulin are not decreased in obese subjects (22, 49). Therefore, the decreased insulin-stimulated glucose uptake found in the enlarged adipocyte is likely to result from a cellular postreceptor defect residing in the glucose transporter proteins (10, 11, 50, 51).

These results show that adipose tissue in obesity is insulin resistant if its metabolic rate is expressed per adipose tissue mass. Adipose tissue has a very specific capacity of increasing its mass by accumulating fat storage. We did not measure the size or weight of adipocytes and can only speculate on the possible cellular metabolic changes in the obese subjects. Obese subjects have shown to have fewer cells in the adipose tissue per gram than their nonobese controls (52). This might explain the finding that the rates of glucose uptake per depot were similar in obese and nonobese. The inverse association between adipose tissue mass measured with MRI and adipose tissue metabolic rate per tissue weight measured directly with [^{18}F]FDG-PET was more exponential than linear (Fig. 5), suggesting that the number of adipocytes was increased in subjects with more severe obesity. In the study of Jansson *et al.* (12), the weight of adipocytes was doubled in abdominal sc in patients with BMI of 39 kg/m^2, compared with lean patients. It may then, based on these measurements, be possible to get an estimate of the glucose uptake per cell number by dividing glucose uptake of a fat depot by a relative number of cells. Because total adipose glucose uptake rates per whole depot were similar in the two subject groups, the assumed difference in the number of adipocytes would mean that glucose uptake per an adipocyte would be about one-third lower in obese, compared with nonobese. This is in accordance with earlier *in vitro* findings (6, 16, 35, 36). Moreover, adipose tissue blood flow has shown to be inversely correlated to cell size (12), indicating that obesity impairs adipose tissue blood flow per mass unit. However, we show here that blood flow in the whole depot is significantly increased in the obese subjects, compared with the nonobese. If we further estimate the blood flow per cell as above, we would end up with a well-reserved blood flow as per cell in abdominal sc region. In accordance, earlier investigation has revealed evidence for a constant blood flow supply per cell in an expanding adipose tissue mass (53).

TABLE 2. Adipose tissue blood flow in various abdominal tissue regions

	Nonobese (n = 10)	Obese (n = 10)	P (t test)
Subcutaneous abdominal fat	4.8 ± 1.0	2.6 ± 0.3	<0.05
Visceral fat	5.9 ± 1.1	3.1 ± 0.1	<0.05
Perirenal fat	4.5 ± 0.7	2.9 ± 0.4	<0.05

Values are expressed as ml/100 g·min^{-1}.

The [^{18}F]FDG-PET technique seems to be suitable for the assessment of metabolic events in different adipose tissue regions *in vivo*. Measurements of adipose tissue and muscle glucose uptake can be performed noninvasively during one session using [^{18}F]FDG-PET under steady-state conditions. Steady-state conditions are required to obtain reliable and constant flux of glucose into the tissue and is therefore a prerequisite of the [^{18}F]FDG-PET method. Because glucose uptake rates were not measured at basal state in our study, it was not possible to quantify the net effect of insulin. A high precision estimate of glucose uptake in the adipose tissue could be obtained because fractional [^{18}F]FDG uptake was calculated using the graphical analysis, and slopes were stochastically scattered with small coefficients of variation in all adipose depots. Furthermore, the lumped constant, LC for [^{18}F]FDG in adipose tissue, was recently measured in our laboratory under identical conditions in humans by comparing [^{18}F]FDG-PET with microdialysis and [^{15}O]-labeled

water. The constant was found to be 1.14 (22), which is close to the LC in skeletal muscle (1.2) determined earlier in three different studies with varying methodology (30, 54, 55). Adipose tissue blood flow was measured using freely diffusible [^{15}O]-labeled water by means of the autoradiographic method previously validated for low perfusion levels (27).

In summary, the results of the present study demonstrate in man *in vivo* the active role of visceral adipose tissue in glucose metabolism. The insulin-stimulated glucose uptake and perfusion are impaired in obesity in all fat depots when expressed per adipose mass unit. However, because of the larger fat mass, total abdominal adipose tissue glucose uptake is not decreased in obese subjects. The contribution of adipose tissue to the whole-body insulin-stimulated glucose uptake is greater than earlier believed, and therapeutic interventions improving glucose disposal in fat depots may substantially affect the whole-body glucose disposal in obese subjects.

Acknowledgments

Received January 24, 2002. Accepted May 8, 2002.

Address all correspondence and requests for reprints to: Pirjo Nuutila, Turku PET Centre, University of Turku, P.O. Box 52, 20521 Turku, Finland. E-mail: pirjo.nuutila@utu.fi.

This work was supported by grants from the Novo Nordisk foundation (to P.N. and P.L.), Finnish Diabetes Research foundation (to K.V. and P.N.), Swedish Diabetes Association (to P.L.), Swedish Research Council (project no. 1084, to P.L.), Finnish Cultural Foundation (to K.V.), and Finnish Association on the Study of Obesity (to K.V.).

References

1. **DeFronzo RA, Gunnarsson R, Bjorkman O, Olsson M, Wahren J** 1985 Effects of insulin on peripheral and splanchnic glucose metabolism in noninsulin-dependent (type II) diabetes mellitus. J Clin Invest 76:149–155
2. **Nuutila P, Knuuti MJ, Heinonen OJ, Ruotsalainen U, Teräs M, Bergman J, Solin O, Yki-Järvinen H, Voipio-Pulkki LM, Wegelius U** 1994 Different alterations in the insulin-stimulated glucose uptake in the athlete's heart and skeletal muscle. J Clin Invest 93:2267–2274
3. **Kissebah AH, Vydelingum N, Murray R, Evans DJ, Hartz AJ, Kalkhoff RK, Adams PW** 1982 Relation of body fat distribution to metabolic complications of obesity. J Clin Endocrinol Metab 54:254–260
4. **Björntorp P** 1990 "Portal" adipose tissue as a generator of risk factors for cardiovascular disease and diabetes. Arteriosclerosis 10:493–496
5. **Mårin P, Andersson B, Ottosson M, Olbe L, Chowdhury B, Kvist H, Holm G, Sjöstrom L, Björntorp P** 1992 The morphology and metabolism of intra-abdominal adipose tissue in men. Metabolism 41:1242–1248
6. **Reaven GM** 1995 Pathophysiology of insulin resistance in human disease. Physiol Rev 75:473–486
7. **Kelley DE, Thaete FL, Troost F, Huwe T, Goodpaster BH** 2000 Subdivisions of subcutaneous abdominal adipose tissue and insulin resistance. Am J Physiol Endocrinol Metab 278:E941–E948
8. **Randle P, Garland PB, Hales CN, Newsholme EA** 1963 The glucose fatty-acid cycle. Lancet 1:785–789
9. **Kolterman OG, Insel J, Saekow M, Olefsky JM** 1980 Mechanisms of insulin resistance in human obesity: evidence for receptor and postreceptor defects. J Clin Invest 65:1272–1284
10. **Pedersen O, Hjollund E, Sorensen NS** 1982 Insulin receptor binding and insulin action in human fat cells: effects of obesity and fasting. Metabolism 31:884–895
11. **Hissin PJ, Foley JE, Wardzala LJ, Karnieli E, Simpson IA, Salans LB, Cushman SW** 1982 Mechanism of insulin-resistant glucose transport activity in the enlarged adipose cell of the aged, obese rat. J Clin Invest 70:780–790
12. **Jansson PA, Larsson A, Smith U, Lönnroth P** 1992 Glycerol production in subcutaneous adipose tissue in lean and obese humans. J Clin Invest 89:1610–1617
13. **Björntorp P, Berchtold P, Holm J, Larsson B** 1971 The glucose uptake of human adipose tissue in obesity. Eur J Clin Invest 1:480–485
14. **Mårin P, Rebuffé-Scrive M, Smith U, Björntorp P** 1987 Glucose uptake in human adipose tissue. Metabolism 36:1154–1160
15. **Coppack SW, Fisher RM, Humphreys SM, Clark ML, Pointon JJ, Frayn, KN** 1996 Carbohydrate metabolism in insulin resistance: glucose uptake and lactate production by adipose and forearm tissues *in vivo* before and after a mixed meal. Clin Sci (Colch) 90:409–415
16. **Jansson PA, Smith U, Lönnroth, P** 1990 Evidence for lactate production by human adipose tissue *in vivo*. Diabetologia 33:253–256
17. **Hagström E, Arner P, Ungerstedt U, Bolinder J** 1990 Subcutaneous adipose tissue: a source of lactate production after glucose ingestion in humans. Am J Physiol 258:E888–E893
18. **Jansson PA, Larsson A, Smith U, Lönnroth, P** 1994 Lactate release from the subcutaneous tissue in lean and obese men. J Clin Invest 93:240–246
19. **Nuutila P, Koivisto VA, Knuuti J, Ruotsalainen U, Teräs M, Haaparanta M, Bergman J, Solin O, Voipio-Pulkki LM, Wegelius U** 1992 Glucose-free fatty acid cycle operates in human heart and skeletal muscle *in vivo*. J Clin Invest 89:1767–1774
20. **Nuutila P, Knuuti MJ, Raitakari M, Ruotsalainen U, Teräs M, Voipio-Pulkki LM, Haaparanta M, Solin O, Wegelius U, Yki-Järvinen H** 1994 Effect of antilipolysis on heart and skeletal muscle glucose uptake in overnight fasted humans. Am J Physiol 267:E941–E946
21. **Nuutila P, Peltoniemi P, Oikonen V, Larmola K, Kemppainen J, Takala T, Sipilä H, Oksanen A, Ruotsalainen U, Bolli GB, Yki-Järvinen H** 2000 Enhanced stimulation of glucose uptake by insulin increases exercise-stimulated glucose uptake in skeletal muscle in humans: studies using [15O]O_2, [15O]H_2O, [18F]fluoro-deoxy-glucose, and positron emission tomography. Diabetes 49:1084–1091
22. **Virtanen KA, Peltoniemi P, Marjamäki P, Asola M, Strindberg L, Parkkola R, Huupponen R, Knuuti J, Lönnroth P, Nuutila P** 2001 Human adipose tissue glucose uptake determined using [^{18}F]-fluoro-deoxy-glucose ([^{18}F]FDG) and PET in combination with microdialysis. Diabetologia 44:2171–2179
23. **Sipilä HT, Clark ML, Peltola O, Teräs M** 2001 An automatic [^{15}O]H_2O production system for heart and brain studies. J Labelled Comp Radiopharm 44(Suppl 1):S1066–S1068 (Abstract)
24. **Hamacher K, Coenen HH, Stocklin G** 1986 Efficient stereospecific synthesis of no-carrier-added 2-[18F]-fluoro-2-deoxy-d-glucose using aminopolyether supported nucleophilic substitution. J Nucl Med 27:235–238
25. **Alenius S, Ruotsalainen U** 1997 Bayesian image reconstruction for emission tomography based on median root prior. Eur J Nucl Med 24:258–265
26. **Numminen P, Tolvanen T, Alenius S, Ruotsalainen U,** New method for calculating attenuation correction factors in PET. Lindberg M, Laine E, eds. Proc XXXIII Annual Conference of the Finnish Physical Society, Turku, Finland, 1999; p. 5.9 (Abstract)
27. **Ruotsalainen U, Raitakari M, Nuutila P, Oikonen V, Sipilä H, Teräs M, Knuuti MJ, Bloomfield PM, Iida H** 1997 Quantitative blood flow measurement of skeletal muscle using oxygen-15-water and PET. J Nucl Med 38: 314–319
28. **Phelps ME, Huang SC, Hoffman EJ, Selin C, Sokoloff L, Kuhl DE** 1979 Tomographic measurement of local cerebral glucose metabolic rate in humans with (F-18)2-fluoro-2-deoxy-D-glucose: validation of method. Ann Neurol 6:371–388
29. **Patlak CS, Blasberg RG** 1985 Graphical evaluation of blood-to-brain transfer constants from multiple-time uptake data generalizations. J Cereb Blood Flow Metab 5:584–590
30. **Peltoniemi P, Lönnroth P, Laine H, Oikonen V, Tolvanen T, Grönroos T, Strindberg L, Knuuti J, Nuutila P** 2000 Lumped constant for [(18)F]fluorodeoxyglucose in skeletal muscles of obese and nonobese humans. Am J Physiol Endocrinol Metab 279:E1122–E1130
31. **Abate N, Garg A, Coleman R, Grundy SM, Peshock RM** 1997 Prediction of total subcutaneous abdominal, intraperitoneal, and retroperitoneal adipose tissue masses in men by a single axial magnetic resonance imaging slice. Am J Clin Nutr 65:403–408
32. **DeFronzo RA, Tobin JD, Andres R** 1979 Glucose clamp technique: a method for quantifying insulin secretion and resistance. Am J Physiol 237:E214–E223
33. **Friedewald WT, Levy RI, Fredrickson DS** 1972 Estimation of the concentration of low-density lipoprotein cholesterol in plasma, without use of the preparative ultracentrifuge. Clin Chem 18:499–502
34. **Durnin JV, Rahaman MM** 1967 The assessment of the amount of fat in the human body from measurements of skinfold thickness. Br J Nutr 21:681–689
35. **Olefsky JM** 1976 The effects of spontaneous obesity on insulin binding, glucose transport, and glucose oxidation of isolated rat adipocytes. J Clin Invest 57:842–851
36. **Lönnroth P, Smith U** 1986 Aging enhances the insulin resistance in obesity through both receptor and postreceptor alterations. J Clin Endocrinol Metab 62:433–437
37. **Kelley DE, Mintun MA, Watkins SC, Simoneau JA, Jadali F, Fredrickson A, Beattie J, Theriault R** 1996 The effect of non-insulin-dependent diabetes mellitus and obesity on glucose transport and phosphorylation in skeletal muscle. J Clin Invest 97:2705–2713
38. **Ciaraldi TP, Molina JM, Olefsky JM** 1991 Insulin action kinetics in adipocytes from obese and noninsulin-dependent diabetes mellitus subjects: identification of multiple cellular defects in glucose transport. J Clin Endocrinol Metab 72:876–882

39. **Garvey WT, Maianu L, Huecksteadt TP, Birnbaum MJ, Molina JM, Ciaraldi TP** 1991 Pretranslational suppression of a glucose transporter protein causes insulin resistance in adipocytes from patients with non-insulin-dependent diabetes mellitus and obesity. J Clin Invest 87:1072–1081
40. **Björntorp P, Sjöström L** 1978 Carbohydrate storage in man: speculations and some quantitative considerations. Metabolism 27(Suppl 2):1853–1865
41. **Rossell R, Gomis R, Casamitjana R, Segura R, Vilardell E, Rivera F** 1983 Reduced hepatic insulin extraction in obesity: relationship with plasma insulin levels. J Clin Endocrinol Metab 56:608–611
42. **Meistas MT, Margolis S, Kowarski AA** 1983 Hyperinsulinemia of obesity is due to decreased clearance of insulin. Am J Physiol 245:E155–E159
43. **Staehr P, Hother-Nielsen O, Levin K, Holst JJ, Beck-Nielsen H** 2001 Assessment of hepatic insulin action in obese type 2 diabetic patients. Diabetes 50:1363–1370
44. **Bonadonna RC, Groop L, Kraemer N, Ferrannini E, Del Prato S, DeFronzo RA** 1990 Obesity and insulin resistance in humans: a dose-response study. Metabolism 39:452–459
45. **Rebuffé-Scrive M, Andersson B, Olbe L, Björntorp P** 1989 Metabolism of adipose tissue in intraabdominal depots of nonobese men and women. Metabolism 38:453–458
46. **Summers LK, Samra JS, Humphreys SM, Morris RJ, Frayn KN** 1996 Subcutaneous abdominal adipose tissue blood flow: variation within and between subjects and relationship to obesity. Clin Sci (Colch) 91:679–683
47. **Bolinder J, Kerckhoffs DA, Moberg E, Hagström-Toft E, Arner P** 2000 Rates of skeletal muscle and adipose tissue glycerol release in nonobese and obese subjects. Diabetes 49:797–802
48. **Larsen OA, Lassen NA, Quaade F** 1966 Blood flow through human adipose tissue determined with radioactive xenon. Acta Physiol Scand 66:337–345
49. **Mokshagundam SP, Peiris AN, Stagner JI, Gingerich RL, Samols E** 1996 Interstitial insulin during euglycemic-hyperinsulinemic clamp in obese and lean individuals. Metabolism 45:951–956
50. **Lönnroth P, Digirolamo M, Krotkiewski M, Smith U** 1983 Insulin binding and responsiveness in fat cells from patients with reduced glucose tolerance and type II diabetes. Diabetes 32:748–754
51. **Bolinder J, Engfeldt P, Östman J, Arner P** 1983 Site differences in insulin receptor binding and insulin action in subcutaneous fat of obese females. J Clin Endocrinol Metab 57:455–461
52. **Hirsch J, Batchelor B** 1976 Adipose tissue cellularity in human obesity. Clin Endocrinol Metab 5:299–311
53. **Digirolamo M, Esposito J** 1975 Adipose tissue blood flow and cellularity in the growing rabbit. Am J Physiol 229:107–112.
54. **Kelley DE, Williams KV, Price JC, Goodpaster B** 1999 Determination of the lumped constant for [18F] fluorodeoxyglucose in human skeletal muscle. J Nucl Med 40:1798–1804
55. **Utriainen T, Lovisatti S, Mäkimattila S, Bertoldo A, Weintraub S, DeFronzo R, Cobelli C, Yki-Järvinen H** 2000 Direct measurement of the lumped constant for 2-deoxy-[1-(14)C]glucose *in vivo* in human skeletal muscle. Am J Physiol Endocrinol Metab 279:E228–E233